Available online at www.sciencedirect.com
ScienceDirect
Journal of Power Sources 174 (2007) 1131–1136
JOURNAL OF POWER SOURCES
www.elsevier.com/locate/jpowsour

Short communication

Effects of Mg-substitution in Li(Ni,Co,Al)O_2 positive electrode materials on the crystal structure and battery performance

H. Kondo [a,*], Y. Takeuchi [a], T. Sasaki [a], S. Kawauchi [a], Y. Itou [a], O. Hiruta [a], C. Okuda [a], M. Yonemura [b], T. Kamiyama [c], Y. Ukyo [a]

[a] *Toyota Central R&D Labs. Inc., Nagakute, Aichi 480-1192, Japan*
[b] *Institute of Applied Beam Science, Graduate School of Engineering and Science, Ibaraki University, 4-12-1 Nakanarusawa, Hitachi, Ibaraki 315-8511, Japan*
[c] *Institute of Materials Structure Science, High Energy Accelerator Research Organization, 1-1 Oho, Tsukuba, Ibaraki 305-0801, Japan*

Available online 26 June 2007

Abstract

Mg-substituted Li(Ni,Co,Al)O_2 have been prepared by a co-precipitation method and examined by XRD, neutron diffraction, X-ray absorption, magnetization and electrochemical measurements. Neutron diffraction measurement indicated that the Mg ions were mostly substituted for Ni ions located in transition metal layers in $LiNi_{0.75}Co_{0.15}Al_{0.05}Mg_{0.05}O_2$. Although a tiny amount of Ni ions in lithium layers in $LiNi_{0.8}Co_{0.15}Al_{0.05}O_2$ was detected by magnetization measurements, such Ni ions decreased by Mg-substitution. The Mg-substitution for Ni in $LiNi_{0.75}Co_{0.15}Al_{0.05}Mg_{0.05}O_2$ was also confirmed by X-ray absorption measurements. The 500 mAh-type cylindrical lithium-ion cells of $LiNi_{0.8-x}Co_{0.15}Al_{0.05}Mg_xO_2$ ($x = 0$, 0.05) with graphite negative-electrode were prepared and their battery performances were evaluated by cycling test at 2 C charge/discharge rate at 60 °C. A lithium-ion cell of $LiNi_{0.75}Co_{0.15}Al_{0.05}Mg_{0.05}O_2$ exhibited better capacity retention and smaller battery resistance than that of $LiNi_{0.8}Co_{0.15}Al_{0.05}O_2$ after 500 cycles. Electrochemical impedance spectroscopy revealed that the Mg-substitution suppressed the increase in charge-transfer resistance upon cycling. The effects of Mg-substitution in $LiNi_{0.8}Co_{0.15}Al_{0.05}O_2$ were discussed in terms of crystal structure and battery performance.

Keywords: Lithium-ion battery; Neutron diffraction; Cycle performance; Electrochemical impedance spectroscopy

1. Introduction

$LiNiO_2$ and its derivatives are the most promising candidates for the positive electrode materials of advanced lithium-ion batteries because of their lower cost and higher capacity compared to those of $LiCoO_2$ [1]. It has been known that the cationic substitution in $LiNiO_2$ is one of the important methods to improve electrochemical reactivity [2]. Among them, Co and Al co-doped $LiNiO_2$-based materials, Li(Ni,Co,Al)O_2, are one of the most applicable materials for automobile-use due to the relatively good thermal stability and cyclability [3–6]. Battery performance of lithium-ion cells of $LiNi_{0.8}Co_{0.15}Al_{0.05}O_2$ has been improved compared to that of $LiNiO_2$ by the effects of Co and Al substitution. However, it has been reported that the lithium-ion batteries of $LiNi_{0.8}Co_{0.15}Al_{0.05}O_2$ still show capacity fading and resistance increase after storage and cycling tests at high temperature [5,6]. In our previous paper [6], we have reported that the increase in resistance of the battery after cycling is confirmed to be mainly attributed to that of the positive electrode, which indicates that innovation in positive electrode materials is necessary to improve battery performance.

In order to suppress the increase in the resistance of positive electrode, we focused on Mg^{2+} ion. Recently, it has been reported that Mg-substitution in $LiNiO_2$ and $LiNi_{1-x}Co_xO_2$ gave the good cyclability even at high temperature and high thermal stability in a charged state [2,7–9]. Pouillerie et al. reported structural and electrochemical properties of $LiNi_{1-y}Mg_yO_2$ [8] and $LiNi_{0.91-y}Co_{0.09}Mg_yO_2$ [9]. They found that the distribution of Mg ions in lithium and transition metal layers is different among these Mg-substituted materials even if the Mg content is the same. Since the battery performance is considered to be strongly affected by the site occupancy of Mg ions as well as that of Ni ions, it is important to determine the site occupancy of substituted cations. In this study, we investigated Mg-substituted $LiNi_{0.8}Co_{0.15}Al_{0.05}O_2$ in order to improve the battery performance in terms of cyclability and resistance increase. The effects

* Corresponding author.
E-mail address: e1261@mosk.tytlabs.co.jp (H. Kondo).

0378-7753/$ – see front matter © 2007 Elsevier B.V. All rights reserved.
doi:10.1016/j.jpowsour.2007.06.035

of Mg-substitution in $LiNi_{0.8-x}Co_{0.15}Al_{0.05}Mg_xO_2$ ($x = 0, 0.05$) is discussed with emphasis on the site occupancy of Mg ions and the battery performance of cylindrical lithium-ion cells with graphite negative-electrode.

2. Experimental

2.1. Structural characterization

$LiNi_{0.8-x}Co_{0.15}Al_{0.05}Mg_xO_2$ ($x = 0, 0.05$) were prepared by a co-precipitation method. The phase purity and structural parameters of these materials were characterized by using X-ray diffraction (XRD) (Rigaku; RINT-TTR) with Cu Kα radiation. The lattice constants were obtained by using least squares method for XRD patterns. Neutron diffraction (ND) measurement was also performed by a time-of-flight (TOF) neutron diffractometer at room temperature, using VEGA and Sirius, at KENS pulsed spallation neutron source at High Energy Accelerator Research Organization (KEK). The collected diffraction data were analyzed by Rietveld method, using the program RIETAN-TN for TOF neutron diffraction [10]. To investigate the presence of Ni ions in lithium layer, magnetization measurements were carried out by a SQUID magnetometer (Quantum Design, MPMS-5) at 6 K in the field range from −5 to +5 T. X-ray absorption fine structure (XAFS) measurements were performed at beam line, No. BL16B2, in spring 8 [11] to determine the average valence of Ni and Co in $LiNi_{0.8-x}Co_{0.15}Al_{0.05}Mg_xO_2$ ($x = 0$, 0.05). Ni and Co *K*-edge XANES spectra were collected and analyzed by using XANADU [12].

2.2. Three electrode test cells

Three electrode cells (Toyo System Co., Ltd.) were fabricated for electrochemical analysis. Li metal was used as a counter electrode and a reference electrode, and 1 M $LiPF_6$ dissolved in an ethylene carbonate (EC) and diethyl carbonate (DEC) solvent (3:7 in volume) was applied as an electrolyte solution. Working electrodes were prepared by casting the slurry composed of 85 wt.% of active materials, 5 wt.% of polyvinylidene fluoride (PVdF) and 10 wt.% of conductive carbon material in the *N*-methyl 2-pyrrolidone (NMP) solvent onto both sides of Al foil. After drying, the electrode sheet was pressed into the appropriate thickness. Cyclic voltammetry was carried out by an electrochemical analyzer (HZ-5000, Hokuto Denko) in the potential range between 3.0 and 4.5 V at a scan rate of 0.2 mV s^{-1} at 20 °C.

2.3. Cylindrical lithium-ion cells

Charge–discharge cycling tests were carried out using 500 mAh-type cylindrical cells with graphite negative-electrode. An outline of the cylindrical cell using in this study was described elsewhere [6]. Positive electrode was prepared by the same method described above. Artificial graphite and 1 M $LiPF_6$ dissolved in an EC and DEC solvent (3:7 in volume) were used as a negative material and an electrolyte solution, respectively. Negative electrode was prepared by casting slurry composed of 95 wt.% of active materials and 5 wt.% of PVdF in the NMP solvent onto both sides of Cu foil.

The cylindrical cells were firstly charged under constant voltage to 4.1 V and discharged at 0.1 C rate to 3.0 V at 20 °C to determine the initial capacity. Battery resistance at 20 °C was obtained from voltage response in relation to the direct current for 10 s. Cycling tests were carried out at a 2 C rate in the range of 3.0 and 4.1 V at 60 °C. Electrochemical impedance spectroscopy (EIS) was performed using the electrochemical analyzer (ALS660B). The impedance spectra were acquired at 3.68 V in frequency range from 100 kHz to 0.01 Hz with the amplitude of 5 mV.

3. Results and discussion

3.1. Materials characterization: crystal and electronic structures

XRD patterns of $LiNi_{0.8-x}Co_{0.15}Al_{0.05}Mg_xO_2$ ($x = 0$, 0.05) were shown in Fig. 1. Single phase, which was *iso*-structural with $LiNiO_2$, was obtained for both samples, and all the peaks were indexed based on the layered α-$NaFeO_2$ structure (space group; $R\bar{3}m$). The lattice constants obtained by using least squares method were also listed in Fig. 1. The *c*-axis parameter of $LiNi_{0.75}Co_{0.15}Al_{0.05}Mg_{0.05}O_2$ was slightly larger than that of $LiNi_{0.8}Co_{0.15}Al_{0.05}O_2$. XRD results suggested that Mg ions were solid-soluted completely without impurity phases in $LiNi_{0.75}Co_{0.15}Al_{0.05}Mg_{0.05}O_2$.

The electrochemical reactivity of Mg-substituted $LiNiO_2$-based materials were associated with distribution of doped Mg in both Li (3b) and Ni (3a) sites based on a space group of $R\bar{3}m$ [2,7–9]. In order to characterize the crystal structure of $LiNi_{0.75}Co_{0.15}Al_{0.05}Mg_{0.05}O_2$ with emphasis on the site occupancy of Li, Ni and doped Mg, ND measurement was performed. The Rietveld refinement was carried out by assuming various

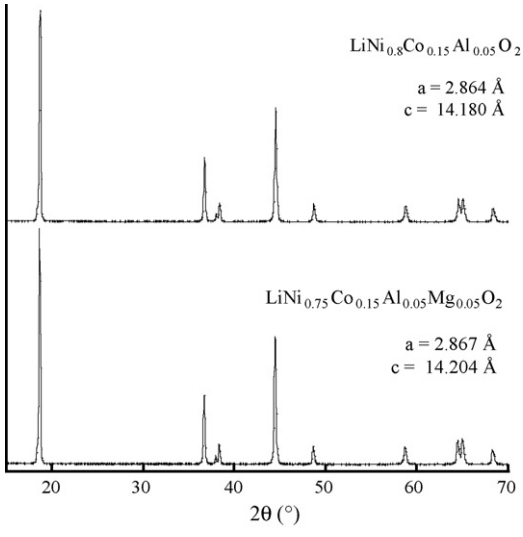

Fig. 1. XRD patterns of $LiNi_{0.8}Co_{0.15}Al_{0.05}O_2$ and $LiNi_{0.75}Co_{0.15}Al_{0.05}Mg_{0.05}O_2$. Lattice constants in the hexagonal manner were obtained by least squares method.

Table 1
Results obtained from the Rietveld refinements for neutron diffraction data of $LiNi_{0.8}Co_{0.15}Al_{0.05}O_2$ and $LiNi_{0.75}Co_{0.15}Al_{0.05}Mg_{0.05}O_2$

Samples	Lattice constants (Å)		Mg occupancy in Ni site (g)	R_{wp}
	a	*c*		
$LiNi_{0.8}Co_{0.15}Al_{0.05}O_2$	2.8645 (1)	14.1847 (2)	–	4.42
$LiNi_{0.75}Co_{0.15}Al_{0.05}Mg_{0.05}O_2$	2.8666 (0)	14.1950 (9)	0.048	4.29

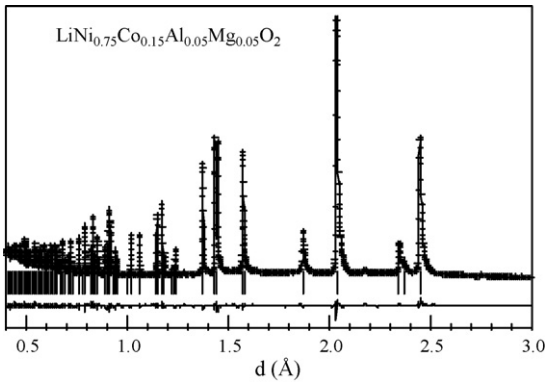

Fig. 2. Neutron diffraction pattern and Rietveld fitting result for $LiNi_{0.75}Co_{0.15}Al_{0.05}Mg_{0.05}O_2$.

refinement models which were considered carefully as taking into account the possibility of cation mixing based on the space group of $R\bar{3}m$. The structural models were constructed under the hypothesis of no vacancies exist in any sites and the fixed Co and Al positions in transition metal layer. The ND pattern and Rietveld refinement results are shown in Fig. 2 and Table 1, respectively. The *c*-axis was expanded by Mg-substitution in $LiNi_{0.75}Co_{0.15}Al_{0.05}Mg_{0.05}O_2$, which was in agreement with XRD results. The converged value of the site occupancy of Li ions exceeded unity assuming that the Ni or Mg existed at lithium layer. Furthermore, the structural model, in which Li ions are distributed at both Ni and Li sites, led to a negative site occupancy for the Li ions at Ni site. These results indicated that $LiNi_{0.75}Co_{0.15}Al_{0.05}Mg_{0.05}O_2$ is a layered structure having no cation mixing. For accuracy, magnetization measurements were carried out at 6 K for $LiNi_{0.8-x}Co_{0.15}Al_{0.05}Mg_xO_2$ ($x = 0$, 0.05) in order to understand the crystal structure in more detail. Rougier et al. have reported for $Li_{1-z}Ni_{1+z}O_2$ system that the Ni ions in lithium layers can be accurately detected by magnetization measurements due to the strong antiferromagnetic interactions between Ni ions in lithium and transition metal layers, that lead to the formation of ferrimagnetic domains [13]. Magnetization measurement revealed that $LiNi_{0.8-x}Co_{0.15}Al_{0.05}Mg_xO_2$ ($x = 0$, 0.05) showed ferromagnetic nature at 6 K, indicating the presence of Ni ions in the lithium layers, while such Ni ions could not be detected by ND measurements. The residual magnetizations of $LiNi_{0.8-x}Co_{0.15}Al_{0.05}Mg_xO_2$ ($x = 0$, 0.05) were listed in Table 2. The residual magnetization of $LiNi_{0.75}Co_{0.15}Al_{0.05}Mg_{0.05}O_2$ was apparently small compared to that of $LiNi_{0.8}Co_{0.15}Al_{0.05}O_2$. This implied that a trace of Ni ions existed in lithium layers in $LiNi_{0.8}Co_{0.15}Al_{0.05}O_2$, and such Ni ions in lithium layers were decreased by Mg-substitution. On the other hand, according to the Rietveld refinement of ND patterns, occupancy (g) of Mg ions in transition metal layers was determined to 0.048 in $LiNi_{0.75}Co_{0.15}Al_{0.05}Mg_{0.05}O_2$ as shown in Table 1. These results suggested that major fraction of doped Mg ions (96% of Mg ions) was located at transition metal layers.

XANES spectra were obtained for $LiNi_{0.8-x}Co_{0.15}Al_{0.05}Mg_xO_2$ ($x = 0$, 0.05), and Ni and Co *K*-edge absorption energies were listed in Table 2. The positions of their *K*-edge absorption energies were decided to be at the half height of jump in the absorption at the threshold energy. While Co *K*-edge absorption energies of both samples were consistent with each other, the Ni *K*-edge absorption energy of $LiNi_{0.75}Co_{0.15}Al_{0.05}Mg_{0.05}O_2$ was higher than that of $LiNi_{0.8}Co_{0.15}Al_{0.05}O_2$. These results mean that the average valence of Ni in $LiNi_{0.75}Co_{0.15}Al_{0.05}Mg_{0.05}O_2$ is higher than that in $LiNi_{0.8}Co_{0.15}Al_{0.05}O_2$ because of charge compensation of Mg^{2+}-substitution for Ni^{3+} ions in transition metal layers and the decrease of Ni ions in lithium layers.

As described above, a single phase of $LiNi_{0.8-x}Co_{0.15}Al_{0.05}Mg_xO_2$ ($x = 0$, 0.05) could be prepared, in which Mg ions were mostly substituted for Ni ions. Although a trace of Ni ions existed in lithium layers in $LiNi_{0.8-x}Co_{0.15}Al_{0.05}Mg_xO_2$ ($x = 0$, 0.05), such Ni ions were decreased by Mg-substitution, suggesting the improved electrochemical reactivity by Mg-substitution in $LiNi_{0.75}Co_{0.15}Al_{0.05}Mg_{0.05}O_2$.

3.2. Materials characterization: electrochemical behavior

In order to reveal the effects of Mg-substitution on the electrochemical behavior, cyclic voltammetry (CV) was performed using three electrode cells with Li metal as reference

Table 2
Magnetization measurements and XAFS results

Samples	Residual magnetization (emu g^{-1})	*K*-edge absorption energy (eV)	
		Ni	Co
$LiNi_{0.8}Co_{0.15}Al_{0.05}O_2$	7.75×10^{-2}	8341.115	7720.065
$LiNi_{0.75}Co_{0.15}Al_{0.05}Mg_{0.05}O_2$	7.78×10^{-3}	8341.229	7720.088

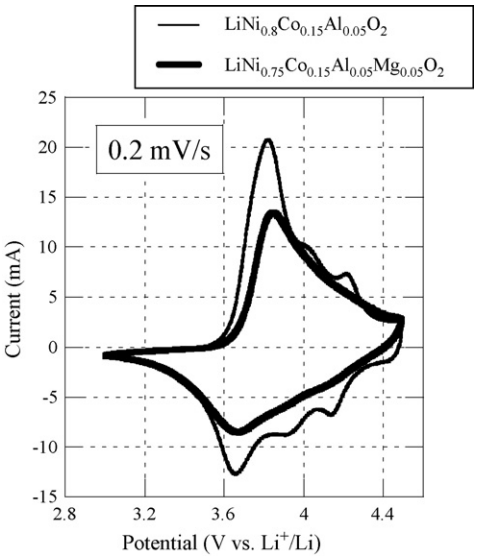

Fig. 3. Cyclic voltammograms of $LiNi_{0.8}Co_{0.15}Al_{0.05}O_2$ and $LiNi_{0.75}Co_{0.15}Al_{0.05}Mg_{0.05}O_2$ with scan rate of 0.2 mV s^{-1}.

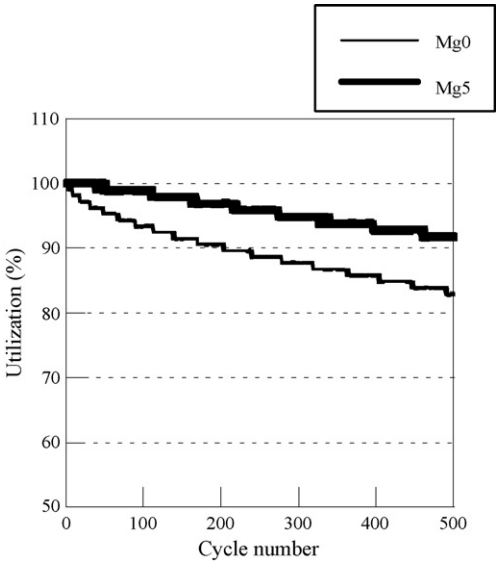

Fig. 4. The specific discharge capacity of the cylindrical lithium-ion batteries of $LiNi_{0.8}Co_{0.15}Al_{0.05}O_2$ and $LiNi_{0.75}Co_{0.15}Al_{0.05}Mg_{0.05}O_2$ with graphite negative-electrode, i.e., Mg0 and Mg5, respectively, at 2 C rate during cycling test at 60 °C.

and counter electrodes. The peak potentials and peak current in the CV curve represent the electrochemical properties of the materials and disclose the phase transitions that occur during (de-)intercalation of Li ions [14]. Cyclic voltammograms were collected in the range between 3.0 and 4.5 V (versus Li^+/Li) at a scan rate of 0.2 mV s^{-1} for three cycles. While the both samples showed large polarization during the first cycle, second and third curves were completely overlapped, indicating good reversible (de-)intercalation of Li ions. Cyclic voltammograms of both samples during the second cycle are shown in Fig. 3. Three broad peaks were observed in cyclic voltammogram of $LiNi_{0.8}Co_{0.15}Al_{0.05}O_2$ on both oxidation and reduction, which were caused by the phase transitions during (de-)intercalation of Li ions [14]. On the other hand, $LiNi_{0.75}Co_{0.15}Al_{0.05}Mg_{0.05}O_2$ showed only single broad peak. These results implied that the phase transitions during (de-)intercalation of Li ions are suppressed by Mg-substitution. It might be considered that the ordering of Li vacancy during (de-)intercalation of Li ions was hindered from phase transitions by presence of Mg ions in transition layers.

3.3. Battery performance

The cylindrical lithium-ion batteries of $LiNi_{0.8}Co_{0.15}Al_{0.05}O_2$ and $LiNi_{0.75}Co_{0.15}Al_{0.05}Mg_{0.05}O_2$ with graphite negative-electrode will be described as Mg0 and Mg5, respectively, hereafter. Fig. 4 shows capacity fading of the batteries during cycling at 2 C rate at 60 °C. The capacity retention of Mg5 after 500 cycles were better than that of Mg0, i.e., 91% for Mg5 and 83% for Mg0 of discharge capacity after 500 cycles compared with the initial capacity, while the initial capacity of Mg5 was slightly lower than that of Mg0. The specific capacity at 20 °C at 0.1 C rate and dc resistance before and after 500 cycles were shown in Fig. 5. Mg5 maintained high specific capacity, 96.5%, even after 500 cycles, whereas the specific capacity of Mg0 was drastically declined to 87% after 500 cycles. In addition, the increase in dc resistance of Mg5 after cycling test was remarkably improved as compared to that of Mg0.

Itou et al. have investigated the origin of the resistance increase of the lithium-ion battery of $LiNi_{0.8}Co_{0.15}Al_{0.05}O_2$ by means of reconstruction method [6]. They clarified that the resistance increase in the battery was mainly attributed to that of the positive electrode. In the present study, to confirm the influence of Mg-substitution on the resistance increase of positive electrode, the electrochemical impedance spectroscopy (EIS) technique was applied to the cylindrical cells. It is known that EIS is a fast, non-destructive and reliable technique which can identify the actual origin of changes in battery resistance [15,16].

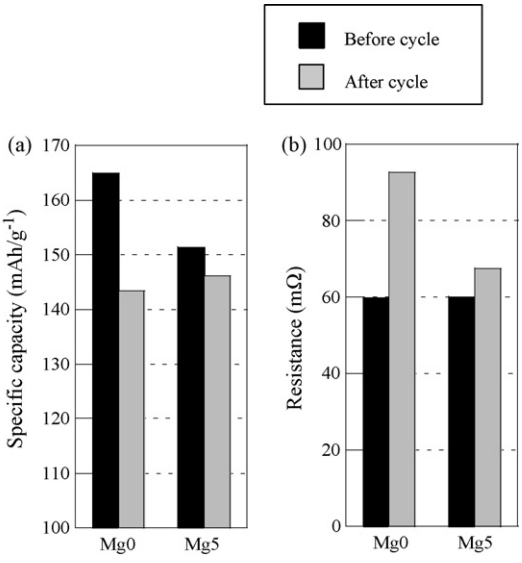

Fig. 5. Graphs of (a) the specific capacity taken at 0.1 C rate and (b) the dc resistance before and after cycles for Mg0 and Mg5 at 20 °C.

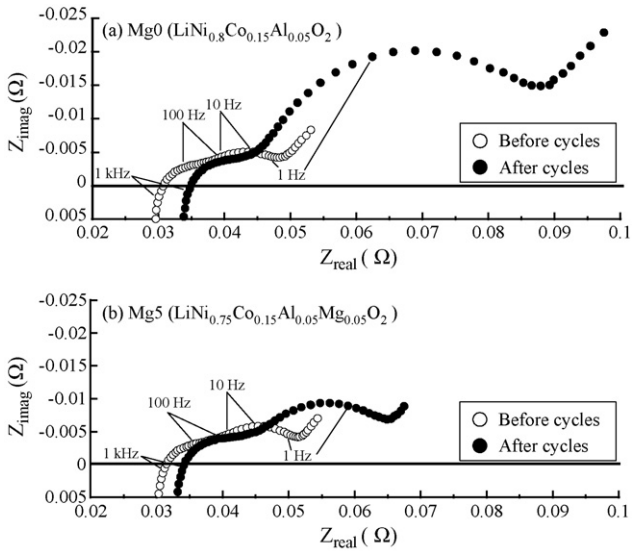

Fig. 6. Nyquist plots of the impedance spectra obtained from (a) Mg0 and (b) Mg5 before and after 500 cycles.

Fig. 6(a) and (b) shows Nyquist plots of the cells at 3.68 V before and after 500 cycles. All Nyquist plots showed typical behaviors of the cylindrical lithium-ion cell, which contained an inductive behavior in the high frequency range followed by two partially overlapped semicircles in the middle and low frequency ranges [16–18]. Some researchers reported a relationship between resistances appeared in the Nyquist plots and individual resistances in the battery [16–18]. We have also confirmed the relationship by comparing the EIS results of Mg0 with half-cell EIS study [18]. The intersection with the real axis in Nyquist plot corresponds to the ohmic cell resistance. Left semicircle resistance in the higher frequency region is interpreted by relaxation of charge carriers in the solid electrolyte interphase (SEI) and charge-transfer resistance of negative electrode, and right semicircle resistance in the lower frequency range is related to the charge-transfer resistance of the positive electrode [17,18]. From the Nyquist plots in Fig. 6(a), right semicircle of Mg0 in the lower frequency range was significantly grown after 500 cycles, while the increase of ohmic and left semicircle resistances was very small. This result indicated that the increase in battery resistance of Mg0 was dominated by increase in the positive electrode resistance, and agreed well with the previous paper [5], and proved a validity of interpretation for the Nyquist plots obtained in this work. As can be seen in Fig. 6(b), the increase in the right semicircle resistance of Mg5 after 500 cycles was suppressed compared to that of Mg0. The increase in the positive electrode resistance after cycling test was remarkably improved only by small amount of Mg-substitution.

From the characterization described in previous sections, it was found that Mg ions can be mostly substituted for Ni ions in transition metal layers in $LiNi_{0.75}Co_{0.15}Al_{0.05}Mg_{0.05}O_2$. Effects caused by Mg-substitution in $LiNi_{0.75}Co_{0.15}Al_{0.05}Mg_{0.05}O_2$ were described as follows. (1) A trace of Ni ions in lithium layers was decreased by Mg-substitution, (2) average valence of Ni ions was increased, and (3) phase transition during (de-)intercalation of Li ions was suppressed. Dokko et al. reported that the phase transitions caused volume changes of $LiNiO_2$ particles accompanied by particle breaking [14]. On the other hand, Itou et al. reported that the cracking of positive electrode materials was one of the degradation mechanisms of lithium-ion batteries due to reducing the paths of electrons and ions in the electrode [6]. We considered that the stability of the layered structure of $LiNi_{0.75}Co_{0.15}Al_{0.05}Mg_{0.05}O_2$ was improved by a presence of Mg^{2+} ions in transition metal layer, which suppressed the phase transition. Thus, the cracking of the particles in the electrode might be suppressed, and the improved cyclability is induced by applying Mg-substituted materials as a positive electrode for lithium-ion batteries. Although the improvement of battery performance seems to be contributed by reducing cation mixing or improving phase stability due to presence of Mg ions, the influences of structural changes caused by Mg-substitution during an electrochemical reaction are still unknown. More examinations are in progress.

4. Conclusions

The effects of Mg-substitution for $Li(Ni,Co,Al)O_2$ on the crystal structure were examined by means of XRD, ND, magnetization measurement, XAFS analysis and CV. Rietveld refinement of ND patterns showed that a major fraction of Mg ions was sitting on transition metal layer. The effects of Mg-substitution on the crystal structure were: (i) reduction of Ni ions in lithium layers, (ii) increase in average valence of Ni ions and (iii) suppression on phase transition during (de-)intercalation of Li ions. The performance of the battery was improved by applying $LiNi_{0.75}Co_{0.15}Al_{0.05}Mg_{0.05}O_2$ as a positive electrode. The capacity retention was improved, namely, 91% of its initial capacity even after 500 charge and discharge cycles at 60 °C. The increase in battery resistance was also reduced by suppressing the increase in charge-transfer resistance of the positive electrode. These improvements of battery performance might be due to the suppression of phase transitions during cycling, which also prevent the particle fracture of positive electrode materials.

Acknowledgement

The authors would like to thank the members of Battery Laboratory (M. Hasegawa, H. Matsuo, and T. Kobayashi) and Nano-analysis Laboratory (Y. Kondo, T. Nonaka and Y. Seno) in Toyota Central R&D Labs. Inc., for valuable discussion and technical supports.

References

[1] K. Sekai, H. Azuma, A. Omaru, S. Fujita, J. Power Sources 43 (1993) 241–244.
[2] C. Delmas, M. Menetrier, L. Croguennec, I. Saadoune, A. Rougier, C. Pouillerie, G. Prado, M. Grune, L. Fournes, Electrochim. Acta 45 (1999) 243–253.
[3] T. Ohzuku, A. Ueda, M. Kouguchi, J. Electrochem. Soc. 142 (1995) 4033–4039.
[4] S. Madhavi, G.V. Subba Rao, B.V.R. Chowdari, S.F.Y. Li, J. Power Sources 93 (2001) 156–162.

[5] C.H. Chen, J. Liu, M.E. Stoll, G. Henriksen, D.R. Vissers, K. Amine, J. Power Sources 128 (2004) 278–285.
[6] Y. Itou, Y. Ukyo, J. Power Sources 146 (2005) 39–44.
[7] C.C. Chang, J.Y. Kim, P.N. Kumta, J. Electrochem. Soc. 147 (2000) 1722–1729.
[8] C. Pouillerie, L. Croguennec, Ph. Biensan, P. Willmann, C. Delmas, J. Electrochem. Soc. 147 (2000) 2061–2069.
[9] C. Pouillerie, F. Perton, Ph. Biensan, J.P. Peres, M. Broussely, C. Delmas, J. Power Sources 96 (2001) 293–302.
[10] T. Ohta, F. Izumi, K. Oikawa, T. Kamiyama, Physica B 234–236 (1997) 1093–1095.
[11] T. Nonaka, C. Okuda, Y. Ukyo, T. Okamoto, J. Synchrotron Rad. 8 (2001) 869–871.
[12] H. Sakane, Proceedings of the 7th German-Japanese Workshop on X-ray Software, 1997.
[13] A. Rougier, C. Delmas, G. Chouteau, J. Phys. Chem. Solids 57 (1996) 1101–1103.
[14] K. Dokko, M. Nishizawa, S. Horikoshi, T. Itoh, M. Mohamedi, I. Uchida, Electrochem. Solid State Lett. 3 (2000) 125–127.
[15] M.D. Levi, G. Salitra, G. Markovsky, H. Teller, D. Aurbach, U. Heider, L. Heider, J. Electrochem. Soc. 146 (1999) 1279–1289.
[16] G. Nagasubramanian, J. Power Sources 87 (2000) 226–229.
[17] D. Aurbach, J. Power Sources 89 (2000) 206–218.
[18] T. Sasaki, K. Horibuchi, H. Kondo, Y. Ito, C. Okuda, O. Hiruta, Y. Takeuchi, Y. Ukyo, K. Tatsumi, S. Muto, Proceedings of the 73rd Meeting of the Electrochemical Society of Japan, 2006, p. 267.